Journal of Alloys and Compounds 504 (2010) 446–451

Contents lists available at ScienceDirect

Journal of Alloys and Compounds

journal homepage: www.elsevier.com/locate/jallcom

X-ray diffraction and Raman spectroscopy on $Gd_2(Ti_{2-y}Te_y)O_7$ prepared at high pressure and high temperature

A.R. Heredia [a], M. Quintana García [b], J.L. Pérez Mazariego [b], R. Escamilla [a,*]

[a] Instituto de Investigaciones en Materiales, Universidad Nacional Autónoma de México, A. Postal 70-360, México D.F. 04510, Mexico
[b] Facultad de Ciencias, Universidad Nacional Autónoma de México, A. Postal 70-360, México D.F. 04510, Mexico

ARTICLE INFO

Article history:
Received 18 September 2009
Received in revised form 26 May 2010
Accepted 29 May 2010
Available online 11 June 2010

PACS:
72.80.Ng
79.60.Ht
07.35.1k
61.10.–i
87.64.Je

Keywords:
Pyrochlores
$Gd_2Ti_2O_7$
High-pressure synthesis
X-ray diffraction
Raman spectroscopy

ABSTRACT

A series of Te-substituted pyrochlores of stoichiometry $Gd_2(Ti_{2-y}Te_y)O_7$ ($y \leq 0.2$) were prepared under high-pressure and high-temperature conditions and characterized by X-ray diffraction, X-ray photoelectron spectroscopy and Raman spectroscopy. X-ray diffraction and X-ray photoelectron spectroscopy studies revealed that the Te^{4+} and Te^{6+} ions occupy the Ti^{4+}sites; the percentage of the contribution of Te^{6+} increases as tellurium content. These substitutions induce an increase of the volume of the TiO_6 octahedron due to the increase in the Ti–O(2) bond length, which preserves the oxygen positional parameter (x_{48f}) and the Gd–O(1) bond length. Results of Raman spectroscopy showed a significant shift to higher frequencies of the E_g mode associated to the O(2) sublattice, as well an increase in the full-width-at-half-maximum intensity (FWHM) of the F_{2g} mode (O–Gd–O bending) as the level of Te substitution for Ti increases. These results are discussed and compared with those reported in the literature.

1. Introduction

Rare earth (RE) pyrochlore materials of the type $A_2B_2O_7$, where A stands for RE and B for a transition metal, have attracted considerable attention in basic science and engineering. As discovered recently, the tetrahedral geometry of cations in pyrochlore exhibits interesting quantum phenomena at low temperature, such as spin ice [1–3] and quantum liquid [4] states. Applications arise, for example, as candidate for radioactive waste disposal and nuclear engineering [5] and potential electrolytes in solid-oxide fuel cells in pyrochlore compounds with intrinsic ionic conduction [6]. The crystal structure of pyrochlores has been described in different ways by many authors [7–10]. Most of these descriptions consider the coordination polyhedra around the A and B cations: the atomic arrangement is completely specified except for the *x* positional parameter for the *48f* oxygen site, which defines the displacement from the ideal fluorite structure. There is no displacement at its minimum value at $x = 0.375$, whereas for $x = 0.4375$, its maximum value, the *48f* site is displaced toward the vacant *8b* site. The phase transition between pyrochlore and defect fluorite structure is driven by the coupled anion occupancy of the *8b* site, which results in a seventh oxygen atom coordinating the B cation, and the creation of an anion vacancy on the *8a* site, resulting in an oxygen deficiency coordination of the A cation [11]. The systematic disordering of both the cation and anion sublattices with increasing *x* has also been confirmed by neutron scattering studies of the closely related pyrochlores, $Y_2(Ti_{1-y}Zr_y)_2O_7$ [12,13] and $Gd_2(Ti_{1-y}Zr_y)_2O_7$ [14,15].

Studies of $A_2B_2O_7$ pyrochlores doped with Te ions have shown that these enter into the structure in either the A sublattice (adopting the oxidation state Te^{4+}) or in the B sublattice (adopting the oxidation state Te^{6+}) [7]. However, the substitution of Te^{4+} ions fully or partially occupying the B sublattice also has been reported [16–18].

Vibrational spectroscopy is ideally suited for the study of crystalline-to-amorphous transitions since there is no requirement for lattice periodicity, unlike diffraction-based techniques. Symmetry analysis of cubic phases such as pyrochlore and fluorite structures, requires that the Raman active and infrared active vibrational modes be mutually exclusive, so several studies of order–disorder transitions in the pyrochlore system have utilized Raman and infrared spectroscopy [19–22].

* Corresponding author.
E-mail address: rauleg@servidor.unam.mx (R. Escamilla).

0925-8388/$ – see front matter © 2010 Elsevier B.V. All rights reserved.
doi:10.1016/j.jallcom.2010.05.143

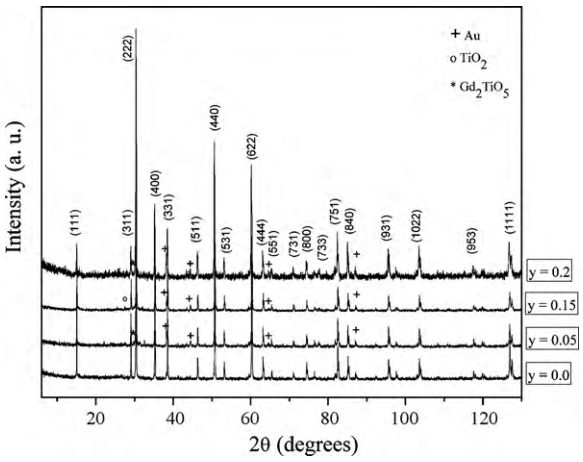

Fig. 1. X-ray diffraction patterns of the $Gd_2(Ti_{2-y}Te_y)O_7$ samples.

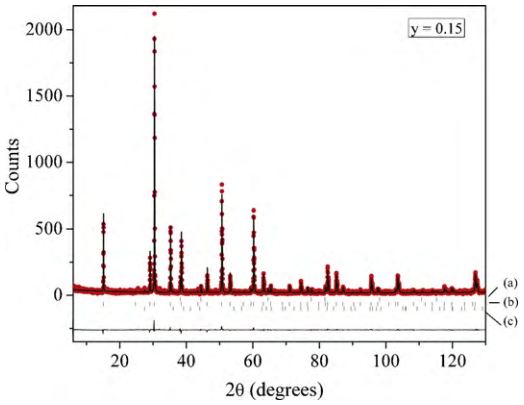

Fig. 2. Rietveld refinement of the X-ray diffraction pattern for $y = 0.15$ sample. Experimental spectrum (dots), calculated pattern (continuous line), their difference (bottom) and the calculated peak positions (middle line). (a) Au, (b) $Gd_2(Ti_{1.85}Te_{0.15})O_7$ and (c) TiO_2 rutile.

In this paper, we describe the Te effect on the crystal structure, the chemical state of Te ions and vibrational modes of pyrochlores of stoichiometry $Gd_2(Ti_{2-y}Te_y)O_7$ ($y \leq 0.2$). The samples were characterized by X-ray diffraction (XRD), X-ray photoelectron spectroscopy (XPS) and Raman spectroscopy.

2. Experimental

Polycrystalline samples of $Gd_2(Ti_{2-y}Te_y)O_7$, with $y = 0$, 0.05, 0.15 and 0.2, were synthesized from starting corresponding oxides, TeO_2, Gd_2O_3 and TiO_2 (99.99% purity) mixed in stoichiometric amounts, sealed in a gold capsule and heated at 900 °C under pressure of 2.1 GPa using a Quickpress piston cylinder press. Phase identification of the samples was done with an X-ray diffractometer Siemens D5000 using Cu K_α radiation and a Ni filter. Intensities were measured at room temperature in steps of 0.02°, in the 2θ range 6–130°. The crystallographic phases were identified by comparison with the X-ray patterns of the JCPDS database. The crystallographic parameters were refined using a Rietveld-fit program, Rietica v 1.71 with multi-phase capability [23].

The chemical analysis was carried out by X-ray photoelectron spectroscopy (XPS). This analysis was performed using a VG Microtech ESCA2000 Multilab UHV system, with an Al K_α X-ray source ($h\nu = 1486.6$ eV), operated at 15 kV and 20 mA beam, and a CLAM4 MCD analyzer. The surface of the pellets was etched for 20 min with 4.5 kV Ar^+ at 0.33 μA mm^{-2}. The XPS spectrum was obtained at 55° to the normal surface in the constant pass energy mode (CAE), $E_0 = 20$ eV for high resolution narrow scan. The peak positions were referenced to the background silver $3d_{5/2}$ photopeak at 368.21 eV, having a FWHM of 1.00 eV, and C 1s hydrocarbon groups in 284.50 eV central peak position. The XPS spectra were fitted with the program SDP v 4.1 [24].

Raman-scattering measurements were performed with a triple Horiba Jobin Yvon T64000 spectrometer equipped with an optical microscope and a photomultiplier tube in a back scattering geometry. A 100× objective was adopted to focus the laser beam of an argon laser (514.5 nm) with a power of 10 mW. Different areas of the samples were measured in order to ensure sample homogeneity. Convolution of the observed bands was done with a Lorentz oscillator model. Fitted curves showed less than 1% error with the corresponding spectra.

3. Results and discussion

3.1. XRD analysis

Fig. 1 shows the powder X-ray diffraction patterns obtained for the system $Gd_2(Ti_{2-y}Te_y)O_7$ type pyrochlore with $y = 0$, 0.05, 0.15 and 0.2. The analysis of these data indicates that the crystal structure of the samples corresponds to $Gd_2Ti_2O_7$ (ICDD no. 73-1698) pyrochlore common structure, although light traces of Gd_2TiO_5 (ICDD no. 21-0342) are observed for the compositions $y = 0.05$ and 0.2, whereas only light traces of TiO_2 (ICDD no. 21-1276) is observed for the sample with $y = 0.15$. Additionally, light traces of Au (ICDD no. 4-0784) are observed in all samples due to the process of synthesis. Mori et al. [25] have shown that the presence of Gd_2TiO_5 or TiO_2 in the pyrochlore $Gd_2Ti_2O_7$ is associated to the effect of vacancies or excess of Gd^{3+} ions in the *16d* sites, respectively.

The X-ray diffraction patterns of the $Gd_2(Ti_{2-y}Te_y)O_7$ samples were Rietveld-fitted using a space group $Fd\bar{3}m$ (No. 227). In the structural refinement we consider the presence of secondary phases and the substitution of Te ions in Ti sites. Fig. 2 shows, as an example, a fitted pattern for $y = 0.15$. Detailed results of the structural refinements are listed in Table 1. In the first two rows we present the evolution of the lattice parameter at room temperature for the $Gd_2(Ti_{2-y}Te_y)O_7$ samples, as function of Te content. It seems that as y is increased, the lattice parameter increases. Fig. 3 shows the evolution of the lattice parameter for the $Gd_2(Ti_{2-y}Te_y)O_7$ samples as a function of Te content (y). For $y = 0$, the lattice parameter was $a = 10.1840(1)$, which is in good agreement with the reported data for $Gd_2Ti_2O_7$ [7].

The increase in the lattice parameter as a function of Te content (y) may be explained considering the coordination number and the ionic radii of the Ti^{4+} and Te^{4+} ions with coordination number 6, in the case of Ti^{4+} the ionic radii is 0.605 Å while that the Te^{4+} is 0.97 Å [26]. From these values, apparently the increase of the unit cell volume may be related to the increase of Te^{4+}, however we cannot discard the possibility of having Te^{6+} in the Ti sites.

Unlike of the substitution of Te ions in the Ti sites, we observed that substituting the Te ions in the Gd sites, in the Rietveld refinement process does not induce significant changes in the quality fitting value of χ^2, therefore we cannot discard this possibility. However, substitution studies with Te^{4+} in the Tl and Te^{6+} in the

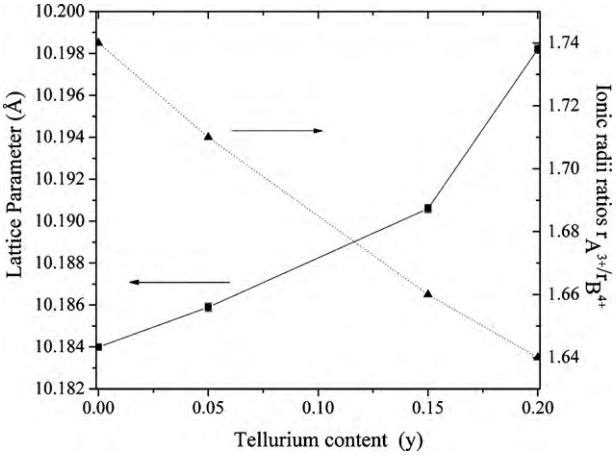

Fig. 3. Crystal lattice parameters and unit cell volume as a function of tellurium content (y).